



OpenAIR@RGU

The Open Access Institutional Repository at Robert Gordon University

<http://openair.rgu.ac.uk>

This is an author produced version of a paper published in

Applied Catalysis B: Environmental (ISSN 0926-3373)

This version may not include final proof corrections and does not include published layout or pagination.

Citation Details

Citation for the version of the work held in 'OpenAIR@RGU':

LIU, I., LAWTON, L. A., BAHNEMANN, D. W. and ROBERTSON, P. K. J., 2005. The photocatalytic destruction of the cyanotoxin, nodularin using TiO₂. Available from *OpenAIR@RGU*. [online]. Available from: <http://openair.rgu.ac.uk>

Citation for the publisher's version:

LIU, I., LAWTON, L. A., BAHNEMANN, D. W. and ROBERTSON, P. K. J., 2005. The photocatalytic destruction of the cyanotoxin, nodularin using TiO₂. *Applied Catalysis B: Environmental*, 60 (3-4), pp. 245-252.

Copyright

Items in 'OpenAIR@RGU', Robert Gordon University Open Access Institutional Repository, are protected by copyright and intellectual property law. If you believe that any material held in 'OpenAIR@RGU' infringes copyright, please contact openair-help@rgu.ac.uk with details. The item will be removed from the repository while the claim is investigated.

The photocatalytic destruction of the cyanotoxin, nodularin using TiO₂.

Iain Liu^a, Linda A. Lawton^b Detlef. W. Bahnemann^c and Peter K. J. Robertson^{a*}

^a *Centre for Research in Energy and the Environment, The Robert Gordon University, Schoolhill, Aberdeen, AB10 1FR.*

^b *School of Life Sciences, The Robert Gordon University, St Andrew Street, Aberdeen, AB25 1HG.*

^c *Institut fuer Technische Chemie, Universitaet Hannover, Callinstrasse 3, D-30167 Hannover, Germany,*

* Corresponding author: Tel: +44-1224-262301; fax: +44-1224-262222.

E-mail address: peter.robertson@rgu.ac.uk (P.K.J. Robertson)

Abstract

Titanium dioxide (TiO₂) photocatalysis has been used to initiate the destruction of nodularin, a natural hepatotoxin produced by cyanobacteria. The destruction process was monitored using liquid chromatography-mass spectrometry analysis which has also enabled the identification of a number of the photocatalytic decomposition products. The reduction in toxicity following photocatalytic treatment was evaluated using protein phosphatase inhibition assay, which demonstrated that the destruction of nodularin was paralleled by an elimination of toxicity.

Keywords: TiO₂, photocatalysis, Nodularin, Cyanotoxin.

1. Introduction.

Cyanobacterial toxins produced and released by cyanobacteria around the world have been well-documented [1,2]. Nodularins (figure 1), produced by the cyanobacterium *Nodularia spumigena*, are structurally and biologically similar to microcystins (figure 2) and both groups of these toxins are among the cyanobacterial toxins usually detected in water [3]. It has been shown that the mode of action of these toxins at a molecular level is caused by the inhibition of serine/threonine protein phosphatases 1 and 2A. Chronic exposure due to the presence of hepatotoxic cyanotoxins in drinking water is thought to be a contributing factor in primary liver cancer (PLC) through the known tumour-promoting activities of these compounds [5-7].

Since cyanobacterial toxins pose a considerable threat to human health, various water treatment processes have been evaluated to degrade these toxins. It is believed, however, that conventional water treatment systems have proven unreliable for the removal of these toxins from water [8,9]. In recent years the use of titanium dioxide (TiO_2) as a photocatalyst for water treatment has been extensively reported. When TiO_2 is illuminated with light of an appropriate wavelength it generates highly active oxidising sites, which can potentially oxidise a large number of organic wastes such as dyes, pesticides, bacteria and herbicides [10-13]. TiO_2 is especially suitable as a photocatalyst for waste treatment, compared to other semiconductors, because it is highly photo-reactive, cheap, non-toxic, chemically and biologically inert, and photostable [14]. Previous work has demonstrated the effectiveness of TiO_2 photocatalysis for the destruction of microcystin-LR in aqueous solutions even at extremely high toxin concentrations, however, a variety of by-products were generated [15,16]. Further mechanistic studies of the process enabled the characterisation of some of the breakdown products and the assessment of their toxicity using protein phosphatase inhibition and brine shrimp bioassays [17,18]. The effectiveness of TiO_2 photocatalysis for destruction of other groups of cyanobacterial toxins such as nodularins has not yet been reported. In this study, we report the destruction of nodularin by TiO_2 photocatalysis. The toxicity of the photocatalytic reaction degradation products has been determined using a protein phosphatase inhibition bioassay.

2. Experimental

2.1. Materials.

Nodularin was obtained from a laboratory culture *Nodularia spumigena* KAC 66 (University of Kalmar, Sweden). Harvested cells were frozen and then extracted in 50% aqueous methanol. The filtered extract was isolated by solid phase extraction followed by separation using preparative HPLC on a C18 column to obtain purified nodularin (18 mg). The purity of the nodularin was subsequently confirmed by comparison to previously purified standards by LC-MS data and by LC photodiode array analysis. Titanium dioxide (Degussa P-25) was used as received. Protein phosphatase 1 was obtained from Sigma, Pool, UK. All other reagents and solvents used were analytical grade or HPLC grade. Aqueous solutions were prepared in Milli-Q water.

2.2. Photocatalysis.

Aqueous solutions (10 ml) of nodularin containing 0.1% (w/v) TiO₂ were illuminated in the presence of air with a 480 W Xenon lamp (Uvalight Technology Ltd.; spectral output 330-450 nm, with light filtered out below 350 nm). The reactions were carried out in glass universal bottles with constant stirring. The distance from the UV lamp to surface of the test solution was 30 cm and the light intensity at this distance was calculated to be 1.91×10^{-5} Einsteins s⁻¹ using ferrioxalate actinometry. On irradiation temperature of the reaction solution stabilised at 30 °C. At timed intervals, samples were taken (0.5 ml) and centrifuged to remove TiO₂ prior to analysis by LC-MS and protein phosphatase inhibition assay. The initial concentration of nodularin was 1 mg ml⁻¹ for the photocatalysis. Controls were performed, both in the dark and in the absence of TiO₂.

2.3. Analysis.

The LC-MS system used in the study was a Waters Alliance 2690 HPLC Pump connected with Waters 996 PDA and Micromass ZQ Mass spectrometer with electrospray ionisation source (Manchester, UK). The HPLC column was a Waters

Symmetry 300TM C18 column (5 μm , 2.1x150 mm, Waters, USA). Treated samples were diluted 10-fold with Milli-Q water before analysis and the injection volume was 10-50 μl . Mobile phases were water and acetonitrile, both containing 0.05% trifluoroacetic acids (TFA). Gradient elution was programmed as 5-20% of acetonitrile in 10 minutes increasing to 80% in 42 minutes. The flow rate was 0.3 ml min^{-1} . The eluent was directly introduced to the mass spectrometer ion source without a splitter. The mass data was obtained in the positive ion mode by full scanning from m/z 150-1000 at a dwell time of 5 seconds with cone voltage at 80eV. Cone induced Dissociation (CID) mass data were obtained by full scanning from m/z 100-1000 at a dwell time of 2 seconds with the cone voltage at 100eV. A Masslynx software workstation was used for the LC-MS instrument control, data acquisition and data processing.

2.4. Protein phosphatase inhibition assay

Protein phosphatase inhibition assay was performed using a modification of previously reported colorimetric procedures.[17, 19-21]. Protein phosphatase 1(PP1) was diluted with buffer containing 50 mM Tris-HCl, 1.0 g l^{-1} BSA, 1.0 mM MnCl_2 and 2.0 mM dithiothreitol, pH 7.4. *p*-Nitrophenyl phosphate (5 mM) was prepared in buffer containing 50 mM Tris-HCl, 20 mM MgCl_2 , 0.2 mM MnCl_2 and 0.5 g l^{-1} BSA, pH 8.1. All buffers were freshly prepared before use. Microcystin-LR, nodularin and test samples were prepared with Milli-Q water. The assay was conducted by addition of 25 μl of test solution to 25 μl of PP1 solution in a 96-well polystyrene microtitre plate. After a few seconds gentle shaking, the microtitre plate was kept at room temperature (c. 22 $^{\circ}\text{C}$) for 5 minutes followed by addition of 200 μl of *p*-nitrophenyl phosphate solution (substrate). The plate was incubated at 37 $^{\circ}\text{C}$ for 60 min. The rate of production of *p*-nitrophenol was measured at 4 minute intervals for 60 minutes at 405nm on a Dynatech MR 5000 Reader. The dose dependent kinetic activity of PP1 against *p*-nitrophenyl phosphate was established to assess the enzyme activity prior to sample test. A standard inhibition curve of microcystin-LR and nodularin was constructed by measuring the percentage inhibition of enzyme activity against a negative control of Milli-Q water. All enzyme assays were performed in triplicate.

3. Results and discussion

When aqueous solutions of nodularin were subjected to TiO₂ photocatalysis, a rapid decomposition of the toxin was observed (figure 3). It can be seen that the reduction of the nodularin peak in the mass chromatogram at 21.76 (figure 3) is accompanied by appearance of new peaks corresponding to decomposition products. On continued irradiation, the nodularin peak rapidly decreased and was no longer detectable after 30 minutes of photocatalysis in a full scan LC-MS mode. The toxicity of the reaction mixture was assessed by protein phosphatase inhibition assay to determine whether the decomposition of nodularin and production of degradation products were paralleled by reduction in toxicity.

The standard inhibition curve (figure 4) of nodularin and microcystin-LR against protein phosphatase 1 demonstrated a nearly 100% inhibition of the enzyme at toxin concentrations over 250 ng ml⁻¹, with a detection limit around 4.0 ng ml⁻¹ for nodularin and 15.7 ng ml⁻¹ for microcystin-LR (20% inhibition). The linear region of the curve appeared between 15.7-62.5 ng ml⁻¹ of the toxins. The concentration that inhibits the enzyme activity by 50% (IC₅₀) level was determined to be around 9 ng ml⁻¹ for nodularin and 45 ng ml⁻¹ for microcystin-LR. Microcystin-LR, therefore appeared to have about 5 times stronger protein phosphatase inhibition activity than nodularin. The IC₅₀ of microcystin-LR and nodularin obtained in this study is in good agreement with that previously reported as 47 ng ml⁻¹ for microcystin-LR and 5.6 ng ml⁻¹ for nodularin [17,22].

Based on the standard inhibition curve, the toxicity of the reaction mixture was assessed. Figure 5 shows that the relative content (bar) of nodularin and the corresponding inhibition (line) against PP1 with irradiation time. It was observed that with the destruction of nodularin following photocatalysis, the enzyme inhibition reduced dramatically after 20 minutes irradiation. After 60 minutes photocatalysis no protein phosphatase inhibition was detectable. This observation indicated that the destruction of nodularin was accompanied by the elimination of toxicity against PP1. The degradation products in the reaction mixture did not show any detectable

inhibition activity against protein phosphatase. The results are similar to those obtained for microcystin-LR decomposition products with photocatalysis [17].

Further characterisation of the by-product peaks were performed using ion extraction techniques. This enabled the preparation of an extracted-ion chromatogram for the process. The extracted-ion chromatogram from full scan TIC of 10 and 20 minutes photocatalysis indicated 11 breakdown product peaks (Table 1). The extracted peak areas from 0 to 100 minutes of photocatalysis were calculated by integration of the peaks in order to demonstrate how the relative amount varied during photocatalysis. Table 1 summarises the peak areas together with their molecular ions and LC retention times. The difference to the levels indicated by “original” and photocatalysis time of 0 min corresponds to dark adsorption of the nodularin to the surface of the photocatalyst; the “original” sample is before the TiO₂ was added and time 0 is where the catalyst has been added but prior to irradiation. As indicated in figure 3 and Table 1, decomposition of nodularin occurred rapidly, after only 2 minutes photocatalysis, degradation was clearly observed. The by-product peaks initially increased during the first 20 minutes irradiation then subsequently decreased with a complete disappearance of all detectable peaks at 100 minutes of photocatalysis. This indicated that the by-products themselves were not stable under photocatalysis and were decomposed further into fragments with mass below the detectable limit for the instrument (<150 Dalton).

Analysis of the full scan mass spectrum of the 11 extracted peaks observed during the photocatalytic degradation of nodularin (Table 1) revealed that all mass spectra of the peaks had their predominant ions with 100% abundance, and were therefore identified as the molecular ions representing the corresponding breakdown products of nodularin. In order to assist in structural elucidation of the by-products, the Cone induced Dissociation (CID) technique was used to obtain fragment information for each of the major peaks obtained from full scan Total Ion Chromatogram (TIC) at cone voltage 80 eV. CID data of the peaks was obtained by increasing the cone voltage to 100eV. The fragment ions associated with nodularin and its by-product peaks were observed at m/z 691, 389, 383, 366, 253, 227 and 135. The CID mass data for nodularin and the observed by-product peaks together with proposed structural assignments [23] are summarised in Table 2. These structure assignments of the

nodularin breakdown products was based on the analysis of the LC-Mass chromatogram and corresponding mass spectrum of by-products (peaks 1-11) assisted by their CID mass data. This data was subsequently used for the elucidation of a proposed mechanism for the photocatalytic destruction process (scheme 1).

In Scheme 1, peak 6 (consisting of peaks 6a-d) was assigned to the dihydroxyl isomers of nodularin resulting from an initial photoisomerisation [24,25] followed by dihydroxylation of the conjugated diene structure system in the Adda side chain. The geometrical isomers share the same molecular ion $[M+H]^+$ at m/z 859 with different LC retention times (16.6-17.9 min) to form the product indicated by peak 6 (a-d). This process appears to be the same as that obtained for microcystin-LR [18], where the Adda diene structure was converted to a (4E), 6(Z) or 4(Z), 6(E) configuration and then formed dihydroxyl products. Since it is impossible to assign the configurations of the isomers to each peak of 6a-6d with LC-MS analysis in this study, precise identity for peaks 6a - 6d could not be assigned.

Following further photocatalytic oxidation, the dihydroxylated Adda bonds were cleaved generating products with peaks 4 and 2, indicated by ion $[M+H]^+$ at m/z 665 and 625 respectively. The product at peak 4 (m/z 665) was further oxidised to form a peroxide product, indicated by peak 3 with ion $[M+H]^+$ at m/z 695 following a peroxidation reaction [26]. Following the peroxide bond cleavage, by-product 3 (peak 3, m/z 695) transformed into by-product 2 (peak 2, m/z 625) on further photocatalysis. It is proposed that mass ion $[M+H]^+$ observed at m/z 286 (peak 1) resulted from the further breakdown product indicated by peak 2 via hydrolysis on the peptide chains of Adda residue-Arg to Glu, and Adda residue-Arg to MeAsp as illustrated in Scheme 1. Adda residue-Arg peptide bond cleavage of this compound at peak 1 resulted in the release of arginine since ion $[M+H]^+$ observed at m/z 175 (peak 7) would be in agreement with this assignment. In the CID mass spectrum (summarised in Table 2), fragment ions at m/z 253, 227 were observed in moderate intensities for peaks 2, 3, 4 and 6. Since m/z 253 was an indication of a moiety of (CO-Glu-Mdhh-H) while ion m/z 227 corresponded to fragments of (Glu-Mdhh+H) or (Mdhh-MeAsp + H), the parent structures (peaks 2, 3, 4 and 6) of these fragments in the nodularin peptide ring appeared to be intact in the early stages of photocatalytic degradation. Moreover, the CID ion at m/z 135, considered to be a characteristic fragment ($\text{PhCH}_2\text{CH}(\text{OCH}_3)$) of

Adda moiety in microcystin or nodularin [23], was absent for peaks 2, 3 or 4 but present for peak 6. This observation would suggest that the isomerised nodularin dihydroxyl products with an Adda moiety and an un-modified Mdhb moiety in peptide ring (peak 6, $[M+H]^+$ at m/z 859) were the precursor of products with peaks 2, 3 and 4.

To summarise, the destruction of nodularin (Scheme 1) therefore appears to be initiated via three processes, ultraviolet (UV) irradiation, hydroxyl radical attack and oxidation [16-18, 27]. UV irradiation induced a geometrical isomerisation of nodularin on the Adda conjugated diene structure to form (4E), 6(Z) or 4(Z), 6(E) Adda configuration. Hydroxyl radical attack decomposed the conjugated diene structure to form the dihydroxylated products. Further photocatalytic oxidation resulted in cleavage of the hydroxylated 4-5 and/or 6-7 bond of Adda to form aldehyde and ketone peptide residues. These by-products subsequently were oxidised to corresponding peroxidated products followed by hydrolysis of peptide bonds forming amino acid fragments.

4. Conclusions

TiO₂ photocatalysis appears to be a highly effective method for the removal of the cyanotoxin nodularin from water. Not only is the nodularin rapidly decomposed by the photocatalytic process, but the toxicity of the toxin is also eliminated. In addition the photocatalytic process effectively destroys the major by-products of the decomposition process with LC-MS detectible products completely degraded within 100 minutes photocatalysis. The major mechanism of the photocatalytic process appears to involve isomerisation, substitution and cleavage of the Adda conjugated diene structure in either nodularin or its resulting derivatives. As the Adda conjugated diene structure in the molecule is believed to be associated with toxicity consequently the toxic effects are eliminated.

Acknowledgements

We are most grateful for the support provided for this work by the European Commission under the Energy, Environment and Sustainable Development programme, contract number EVK1-CT-2000-00077.

References

- [1] W.W. Carmichael, in: G.M. Hallegraeff, D.M. Anderson, A.D. Cembella (Eds.) *Manual on Harmful Marine Microalgae*, United Nations Educational, Scientific and Cultural Organization; Paris, 1995
- [2] K. Sivonen, *Phycologia*. 35 (1996) 12-24.
- [3] K. Sivonen, W.W. Carmichael, M. Namikoshi, K.L. Rinehart, A.M. Dahlem, S.I. Niemela, *Appl. Environ. Microbiol.* 56 (1990) 2650-2657.
- [4] J. Dunn, *Brit. Med. J.* 312 (1996) 1183-1184.
- [5] S.Z. Yu, in: D.A. Steffensen, B.C. Nicholson (Eds.) *Toxic cyanobacteria, Current status of Research and Management*, Australia Centre for Water Quality Research, Salisbury, Australia, 1994.
- [6] S. Yoshizawa, R. Matsushima, M.F. Watanabe, K. Harada, A. Ichihara, W.W. Carmichael, H. Fujiki, *J. Cancer. Res. Clinic. Oncol.* 116 (1990) 609-614.
- [7] M. Namikoshi, K.L. Rinehart, R. Sakai, R.R. Stotts, A.M. Dahlem. V.R. Beasley, W.W. Carmichael, W.R. Evans, *J. Org. Chem.* 57 (1992) 866-872.
- [8] K. Lahti, L. Hiisvirta, *Water Supply*. 7 (1989) 149-154.
- [9] A.M. Keijola, K. Himberg, A.L. Esala, K. Sivonen, L. Hiisvirta, *Toxicol. Assess.* 3 (1988) 643-656.
- [10] M. R. Hoffmann, S. T. Martin , W. Choi, D. F. Bahnemann , *Chem. Rev.* 95 (1995) 69.
- [11] L. Linsebigler, G. Lu, J. T. Yates Jr., *Chem. Rev.* 95 (1995) 735.
- [12] P. K. J. Robertson, *J. Cleaner Prod.* 4 (1996) 203.
- [13] A. Mills, S. Morris, *J. Photochem. Photobiol. A: Chem.* 71 (1993) 75.
- [14] Mills, R. H. Davies, D. Worsley, *Chem. Soc. Rev.* (1993) 417.

- [15] P.K.J. Robertson, L.A. Lawton, B. Munch, J. Rouzade, *Chem. Comm.* 4 (1997) 393-394.
- [16] L.A. Lawton, P.K.J. Robertson, B.J.P.A. Cornish, M. Jaspars, *Environ. Sci. Technol.* 33 (1999) 771-775.
- [17] I. Liu, L.A. Lawton, B.J.P.A. Cornish, P.K.J. Robertson, *J. Photochem. Photobiol. A. Chem.* 148 (2002) 349-354.
- [18] I. Liu, L.A. Lawton, B.J.P.A. Cornish, P.K.J. Robertson, *Environ. Sci. Technol.* 37 (2003) 3214-3219.
- [19] J. An, W.W. Carmichael, *Natural Toxins* 7 (1999) 377-385.
- [20] J. An, W.W. Carmichael, *Toxicon* 32 (1994) 1495-1507.
- [21] C.J. Ward, K.A. Beattie, E.Y.C. Lee, G.A. Codd, *FEMS Microbiology Letters* 153 (1997) 465-473.
- [22] J. Dahlmann, A. Ruhl, C. Hummert, G. Liebezei, P. Carlsson, E. Granéli, *Toxicon* 39 (2001) 1183-1190.
- [23] M. Namikoshi, B.W. Choi, R. Sakai, F. Sun, K.L. Rinehart, W.W. Carmichael, W.R. Evans, P. Cruz, M.H.G. Munro, J.W. Blunt, *J. Org. Chem.* 59 (1994) 2349-2357.
- [24] K. Kaya, T. Sano, *Chem. Res. Toxicol.* 11 (1998) 159-163.
- [25] K. Tsuji, T. Watanuki, F. Kondo, M. Watanabe, S. Suzuki, H. Nakazawa, M. Suzuki, H. Uchida, K. Harada, *Toxicon* 33 (1995) 1619-1631.
- [26] H. Gilman, R. Adams, H.T. Clarke, H. Adkins, C.S. Marvel, *Organic Chemistry, An advanced Treatise, Second Edition, Volume I*, John Willey & Sons, New York, 1947.
- [27] L.A. Lawton, P.K.J. Robertson, B.J.P.A. Cornish, *J. Porphyrins Phthalocyanines* 3 (1999) 544-551

List of Captions for Figures.

Figure 1. Nodularin.

Figure 2. Generic structure of microcystins where X and Z represent the variable amino acids and, D-Me-Asp is *D-erythro-β*-methylaspartic acid, Adda is (2*S*, 3*S*, 8*S*, 9*S*)-3-amino-9-methoxy-2,6,8-trimethyl-10-phenyldeca-4(*E*),6(*E*)-dienoic acid, D-Glu is *D*-glutamic acid and Mdha is *N*-Me-dehydroalanine.

Figure 3. Total Ion Chromatograms (TIC) of the breakdown of nodularin following TiO₂ photocatalysis

Figure 4. Standard inhibition curve of microcystin-LR and nodularin against protein phosphatase (PP1),

Figure 5. Destruction of nodularin (bar) and elimination of protein phosphatase inhibition (line) following photocatalysis with TiO₂. Each point plotted for PP1 inhibition is the means of 3 observations, and the vertical bars indicate the standard deviation (STDEV) of the means.

Table 1. Peak area (counts x 10⁵) of nodularin degradation products detected with LC-MS

Table 2. ESIMS/CID/MS data for nodularin degradation products

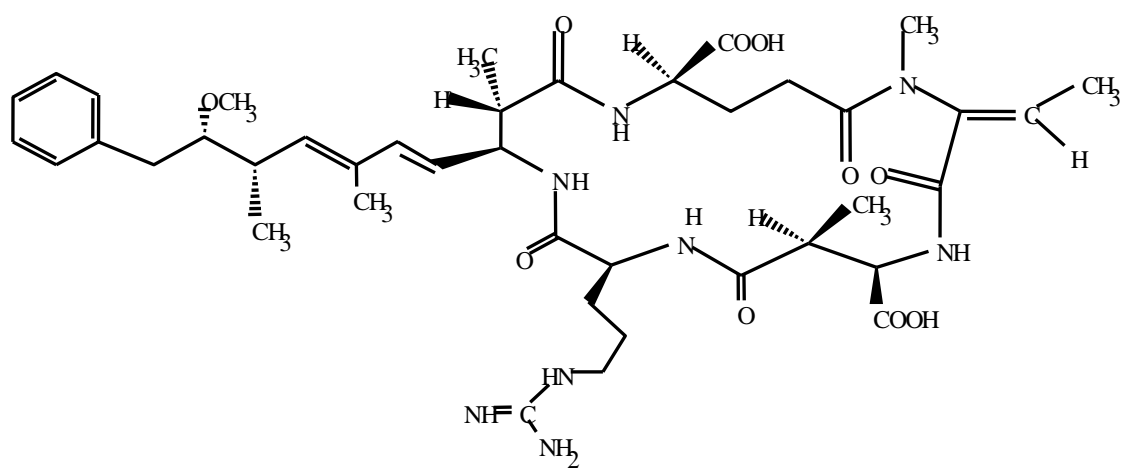


Figure 1.

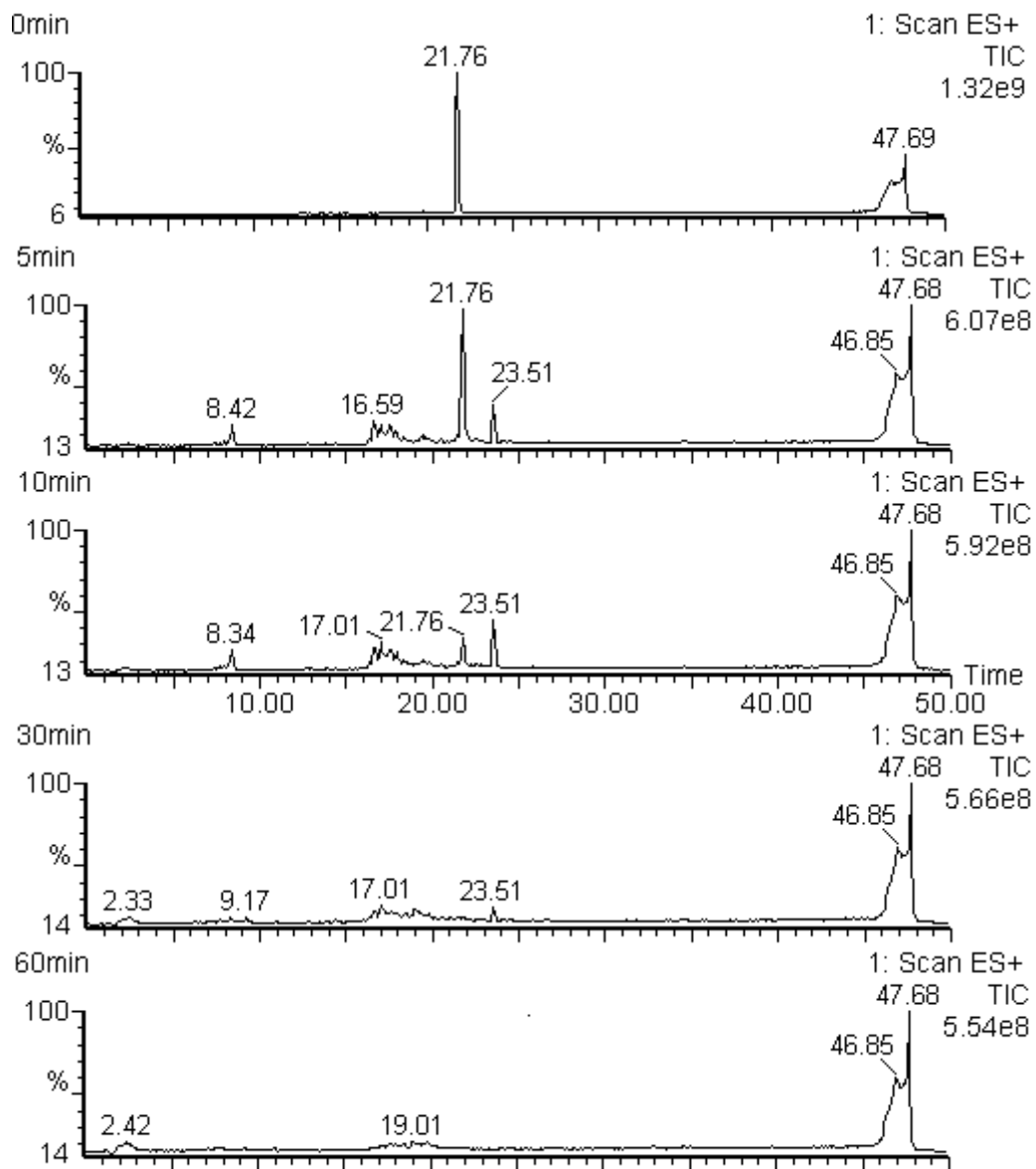


Figure 3.

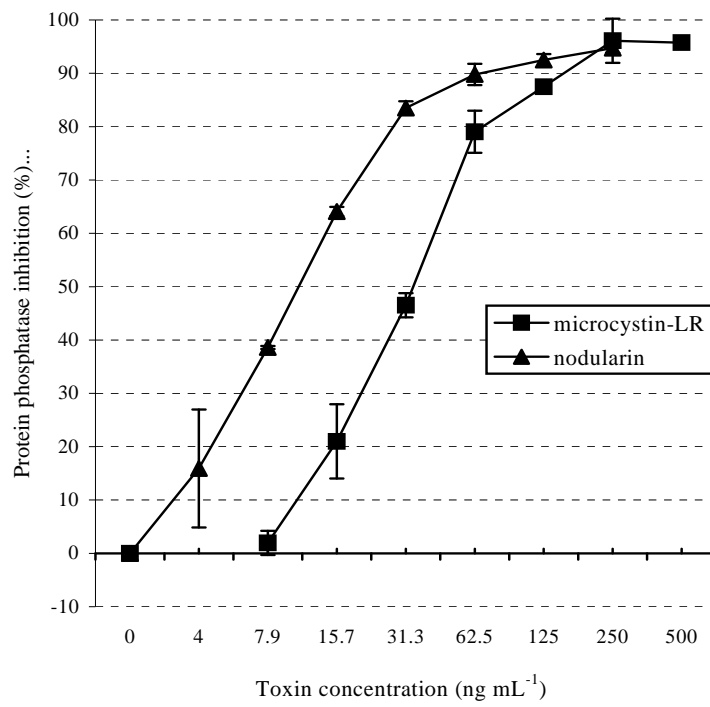


Figure 4

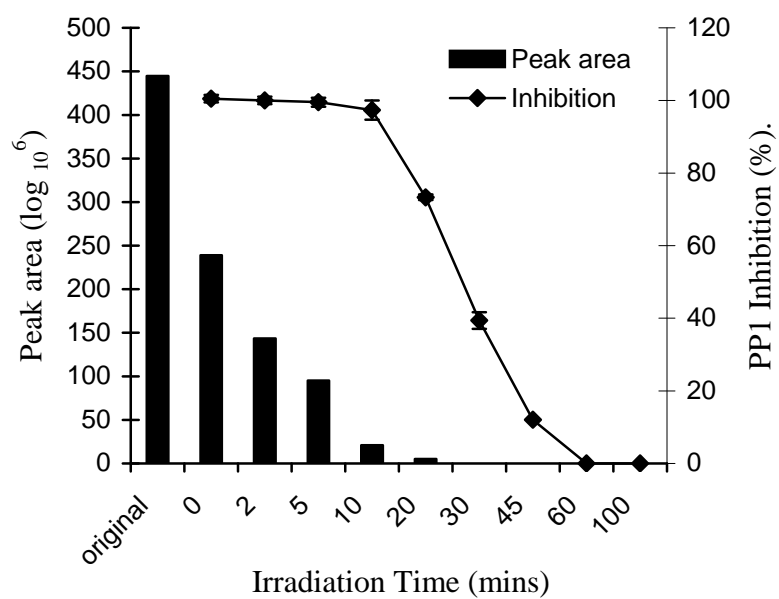


Figure 5.

Nodularin degradation scheme 1.

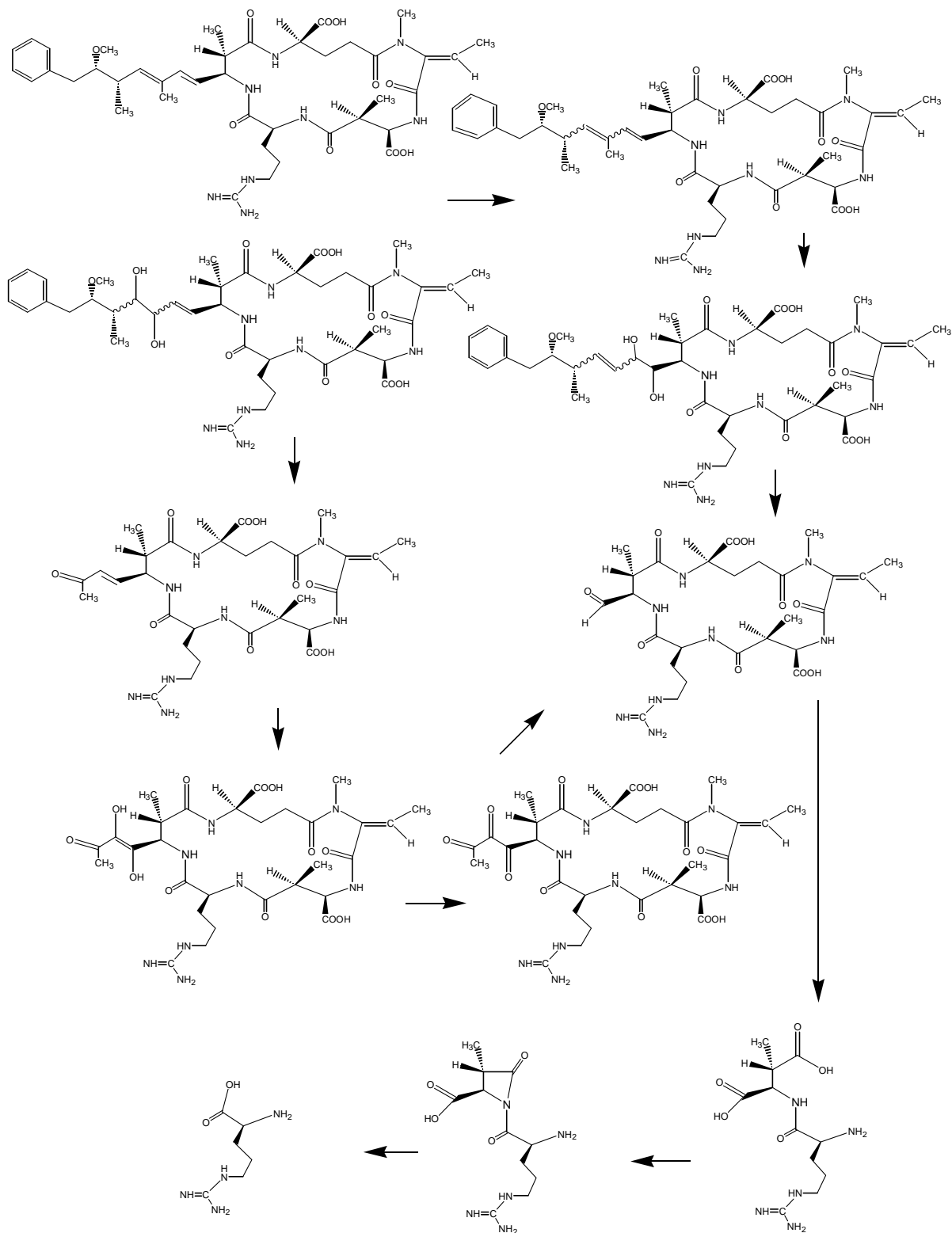


Table 1.

Time (min) of photocatalysis	peak name	1	2	3	4	5*	6*	7	8*	9	10	11	nodularin
	RT(min)	2.0-2.1	7.7	8.3	8.3-8.4	9.2-10.9	16.6-17.9	16.6-17.2	18.5-19.7	21.4-21.5	21.9-22.0	23.5-23.6	21.7-21.8
	M+H(m/z)	286	625	695	665	635	859	175	829	797	811	795	825
original		0	0	0	0	0	0	0	0	0	0	0	1724.4
0		0	0	0	0	0	0	0	0	0	0	0	908.7
2		2.7	1.7	5.3	9.3	0	13.6	8.4	0	2.6	0	23.3	516.2
5		5.5	2.4	7.8	17.9	0	17.6	11.7	0	6.5	0	43.2	318.1
10		8.3	1.0	12.2	19.3	1.1	25.2	13.5	4.7	8.2	0	58.3	44.6
20		13.3	0	8.4	7.5	1.9	20.0	11.4	13.4	4.8	2.8	35.7	0
30		8.8	0	3.1	1.5	2.4	11.1	5.8	9.0	2.4	4.1	14.4	0
45		6.7	0	0	0	1.9	3.1	2.2	8.2	1.0	3.5	5.0	0
60		7.5	0	0	0	1.2	0	0	7.7	0	2.8	0	0
100		0	0	0	0	0	0	0	0	0	0	0	0

* Multiple-peaks with area cited here for principal peak

Table 2.

Fragment formula	ion	Peak name	1	2	3	4	5*	6*	7	8*	9	10	11	nodularin
		RT(min)	2.0- 2.1	7.7	8.3	8.3- 8.4	9.2- 10.9	16.6- 17.9	16.6- 17.2	18.5- 19.7	21.4- 21.5	21.9- 22.0	23.5- 23.6	21.7-21.8
		M+H(m/z)	286	625	695	665	635	859	175	829	797	811	795	825
M - 135 + H	691		-	-	-	-	-	-	-	-	-	nt	-	691
C11H15O-Glu-Mdhb	389		-	-	-	-	-	-	-	-	-	nt	-	389
Mdhb-MeAsp-Arg+H	383		-	-	-	-	-	-	-	-	-	nt	-	383
Mdhb-MeAsp-Arg+H- OH	366		-	-	-	366	-	366	-	-	-	nt	-	366
CO-Glu-Mdhb - H	253		-	253	253	253	-	253	-	-	-	nt	-	253
Glu-Mdhb +H / Mdhb-MeAsp + H	227		-	227	227	227	-	227	-	-	-	nt	-	227
PhCH2CH(OCH3)	135		-	-	-	-	-	135	-	135	135	nt	135	135

* Multiple-peaks with CID ions cited for the largest peak
nt. not tested